Dynamic Response of a Pendulum-Driven Energy Harvester in the Presence of Noise

M Borowiec[1], G Litak[1], A Rysak[1], P D Mitcheson[2], and T T Toh[2]

[1] Lublin University of Technology, Nadbystrzycka 36, 20-618 Lublin, Poland
[2] Department of Electrical and Electronic Engineering, Imperial College London, London SW7 2AZ, UK

E-mail: m.borowiec@pollub.pl

Abstract. This paper presents time- and frequency-domain analyses of a previously reported wave energy harvesting system in the presence of noise. The energy harvester comprises a pendulum that drives two DC generators connected electrically in series. A mechanical model of the wave energy harvester is developed and simulated in Matlab. The output voltage and output power of the energy harvester is evaluated and compared for two input signal types: a deterministic case and a stochastic case. The latter consists of a white noise random excitation source that is bounded in amplitude at a fixed standard deviation. Simulation results indicate that a stochastic input signal shows considerable influence on the output characteristics of the energy harvester. The simulation models developed in this paper can be used to complement the design of resonant frequency tuning electronics for energy harvesting systems.

1. Introduction

The presence of noise within the source excitation frequency will degrade the performance of an energy harvesting system that is designed to operate at its mechanical resonant frequency. This is evident in practical applications, whereby the source vibration frequency may have additional time varying and sometimes stochastic components [1, 2]. Tuning the resonant frequency of such energy harvesters have been demonstrated mechanically [3] or electronically [4, 5]. However, those methods were implemented under sinusoidal input excitations.

In this paper, which is an extension of the work reported in [5, 6], we will discuss the behaviour and efficiency of the electronic tuning circuit in the presence of stochastic excitations. The tuning circuit is represented by a parallel combination of a resistor, capacitor and inductor which are connected across two DC generators connected electrically in series to increase the generated voltage. A photograph of the setup is shown in figure 1(a) and this prototype was designed to be deployed in an unmanned surface vehicle (USV).

2. Mathematical model

A mathematical model of the pendulum-driven energy harvester is given by equation (1).

$$\ddot{\theta} = -d\dot{\theta} + b\Omega^2 \sin\left(\Omega t + \Gamma\left(t\right)\right) - aI_L - c\sin\left(\theta + b\sin\left(\Omega t + \Gamma\right)\right) \tag{1}$$

where a, b, c and d are constants, θ is the relative angular displacement between the pendulum and frame, $\dot{\theta}$ is the angular velocity, $\ddot{\theta}$ is the angular acceleration and Ω is the input excitation

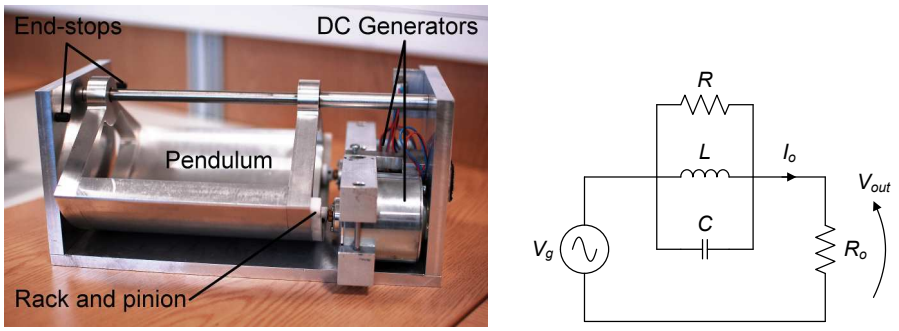

(a) (b)

Figure 1. Photograph and electrical equivalent circuit of the pendulum-driven energy harvesting system.

frequency, $2\pi f$. Finally, $\Gamma(t)$ is a time-dependent, Gaussian distributed white noise component which is introduced into the mechanical system [7, 8] through the input excitation signal Ψ which is defined in equation (2).

$$\Psi(t) = b\sin(\Omega t + \Gamma(t)) \tag{2}$$

Figure 1(b) shows the electrical equivalent circuit of the DC generators, a synthesised RLC impedance to represent an electronic tuning circuit and an output resistor R_o to represent a load application. The generated voltage V_g from the DC generators is given by equation (3).

$$V_g = K_e\dot{\theta} \tag{3}$$

The output current I_o is expressed in equation (4), where K_e is the motor constant of the DC generators and R, L and C represents the synthesised load resistance, inductance and capacitance respectively. The armature inductance of the DC generators can be neglected because the pendulum's oscillation frequency is typically less than 2 Hz for the intended application in an USV. For simplicity, the armature resistance was grouped with R_o.

$$I_o = \frac{V_g - V_{out}}{R} + C\frac{\mathrm{d}}{\mathrm{d}t}(V_g - V_{out}) + \frac{1}{L}\int_0^t (V_g - V_{out})\,\mathrm{d}t \;;\; V_{out} = I_o R_o \tag{4}$$

3. Numerical simulations

Matlab simulations of equations (1), (3) and (4) were performed using the Euler-Maruyama algorithm [9]. Two types of input excitation signals, $\Psi(t)$, were used: a harmonic signal and a stochastic signal with standard deviation $\sigma_\Gamma = 0.4\mathrm{rad}/\sqrt{s}$. This type of stochastic signal was previously investigated in [7, 8] and the time- and frequency-domain plots of the signal is shown in figure 2(c) and figure 2(d). The parameters used in the simulations are listed in table 1.

The output voltage V_{out} across a 1 kΩ output resistor, from a deterministic input signal and from a stochastic input signal is presented in figure 3. The time-domain plots of the input signals are on the left whereas the graphs on the right are their Fourier-transformed equivalents.

The phase portraits of the pendulum under harmonic and stochastic input excitations are shown in figure 4. As expected, the harmonic (deterministic) case shows a symmetrical phase portrait centred at the origin. Whereas for the stochastic excitation case, the phase portrait shows an open and wandering trajectory.

The instantaneous output power for the two input signals are shown in figure 5, with the stochastic case demonstrating large and non-harmonic fluctuations. Interestingly, the average

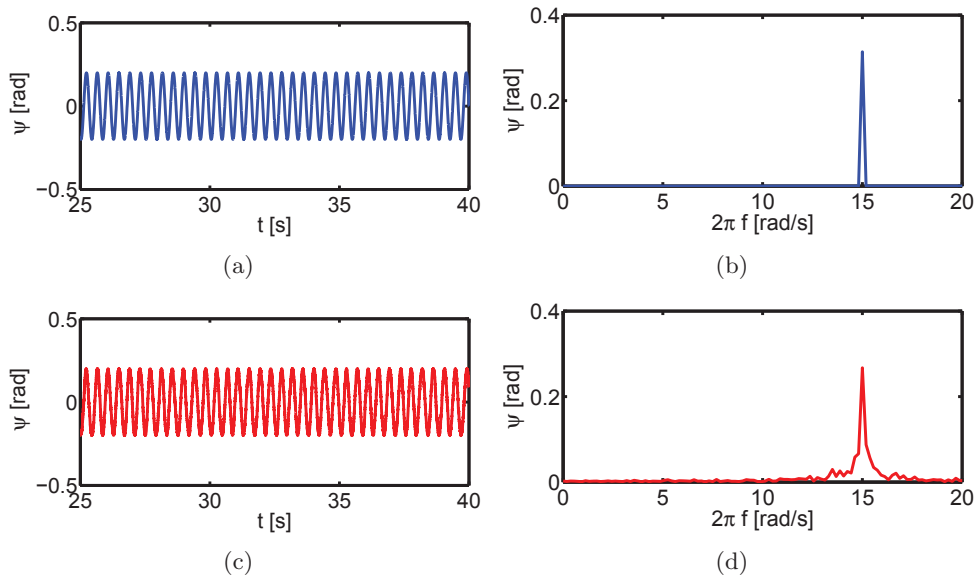

Figure 2. A harmonic signal (top) and a stochastic signal (bottom) were used as the input. Note that time-domain signals are not identical and this can be confirmed by comparing their respective frequency spectra.

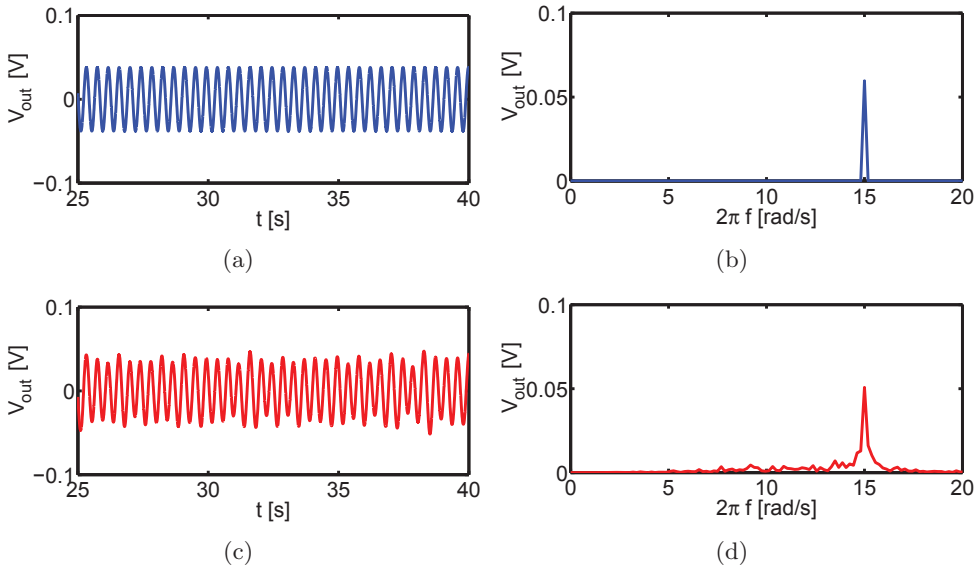

Figure 3. Time- and frequency-domain responses of the output voltage V_{out} for a harmonic (top) and stochastic (bottom) input signals. In the latter, σ_Γ is 0.4 rad/$\sqrt{s}$.

output power for the deterministic and stochastic cases are similar: 0.66 μW and 0.69 μW respectively.

Figure 6 shows the variation of average output power against output resistance at three values of σ_Γ. The results for the periodic and stochastic cases are very similar but upon further inspection, the stochastic case appears to be more efficient. This could be due to $\Gamma(t)$ having a random phase which contributes additional excitation frequencies. Consequently, this increases the available energy from the pendulum that can be harvested by the DC generators.

Table 1. List of simulation parameters and values.

Parameter	Value	Parameter	Value
a	0.6 rad·s^{-2}/A	R	50 Ω
b	0.2 rad^{-1}	L	10 mH
c	79.8 rad·s^{-2}	C	1 mF
d	2.3 s^{-1}	R_o	1 kΩ
Ω	15 rad·s^{-1}	K_e	13 mV/rad·s^{-1}

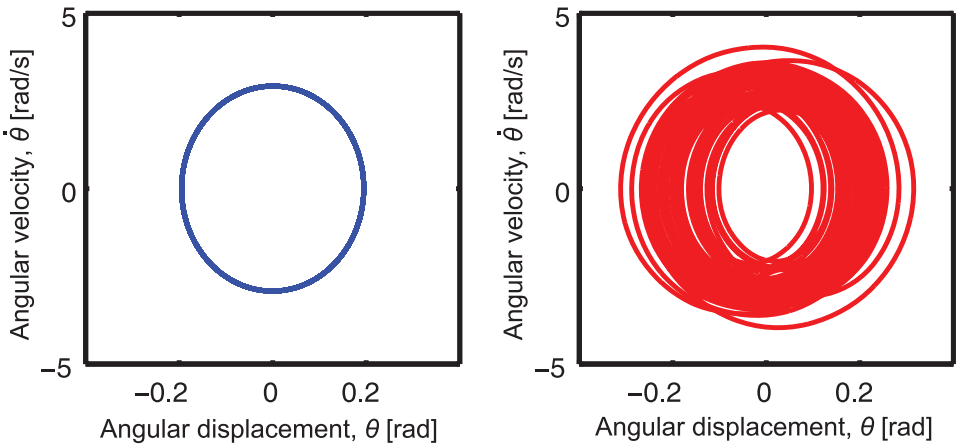

(a) (b)

Figure 4. Phase portraits of the pendulum for: (a) deterministic and (b) stochastic input signals. The standard deviation σ_Γ is 0.4 rad/$\sqrt{s}$.

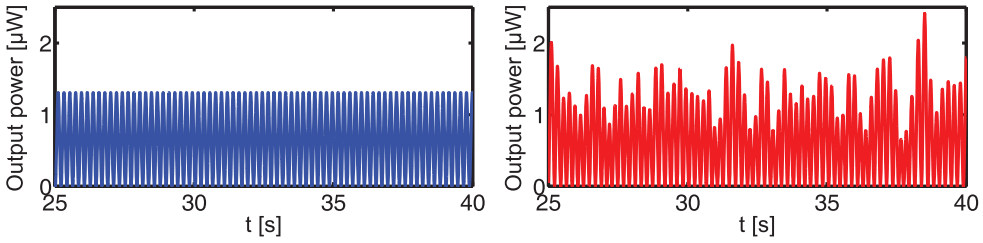

(a) (b)

Figure 5. Instantaneous output power from a deterministic (left) and a stochastic (right) input signal.

4. Conclusions

A comparison of the output characteristics of a pendulum-driven energy harvester was performed using a harmonic and a stochastic input signal. The results show considerable influence of the noise component on the output voltage. The simulated average output power in both cases is similar and this is because of the small σ_Γ. This work demonstrated that, under stochastic excitations, the average output power is slightly higher compared to the deterministic case and

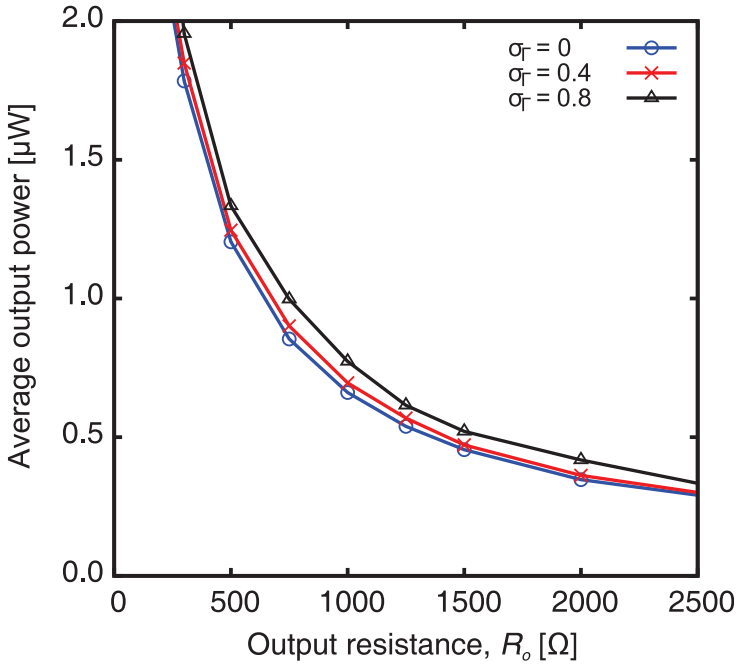

Figure 6. Average output power of the harmonic ($\sigma_\Gamma = 0.0$, circles) and stochastic ($\sigma_\Gamma = 0.4$, crosses & $\sigma_\Gamma = 0.8$, triangles) excitation cases versus the output resistance R_o.

even more so at larger σ_Γ values for the parameters used in the simulations. Further work is needed to establish the parameters of a Gaussian distributed input noise that will affect the output power generation of an energy harvester. Such an analysis will complement the design of a controller that can accurately determine the appropriate synthesised load impedance for stochastic excitation conditions.

Acknowledgements
This work is supported by The Royal Society International Exchanges Scheme, reference number: IE130292.

References

[1] Beeby S P, Wang L, Zhu D, Weddell A S, Merrett G V, Stark B, Szarka G and Al-Hashimi B M 2013 *Smart Mater. Struct.* **22** 075022
[2] Neri I, Travasso F, Mincigrucci R, Vocca H, Orfei F and Gammaitoni L 2012 *J. Intell. Mater. Syst. and Struct.* **23** 2095–2101
[3] Ayala-Garcia I N, Zhu D, Tudor M J and Beeby S P 2010 *Smart Mater. Struct.* **19** 115005
[4] Cammarano A, Burrow S G, Barton D A W, Carrella A and Clare L R 2010 *Smart Mater. Struct.* **19** 055003
[5] Mitcheson P D, Toh T T, Wong K H, Burrow S G and Holmes A S 2011 *IEEE Trans. Circuits and Systems II* **58** 792–796
[6] Toh T T, Mitcheson P D, Dussud L, Wright S W and Holmes A S *Proc. PowerMEMS 2011* pp 383–386
[7] Litak G, Borowiec M and Wiercigroch M 2008 *Dynamical Systems* **23** 259–265
[8] Kwuimy C A K, Litak G, Borowiec M and Nataraj C 2012 *Appl. Phys. Lett.* **100** 024103
[9] Naess A and Moe V 2000 *Probabilistic Engineering Mechanics* **15** 221–231